JOC The Journal of Organic Chemistry

White Light Induced E/Z-Photoisomerization of Diphenylamine-tethered Fluorescent Stilbene Derivatives: Synthesis, Photophysical and Electrochemical Investigation

shachi mishra, Pallavi Awasthi, Jagriti Singh, Rahul K Gupta, Vikram Singh, Ruchir Kant, Ram Jeet, Debabrata Goswami, and Atul Goel

J. Org. Chem., **Just Accepted Manuscript** • DOI: 10.1021/acs.joc.8b00033 • Publication Date (Web): 09 Mar 2018

Just Accepted

ACS Publications

is published by the American Chemical Society. 1155 Sixteenth Street N.W., Washington, DC 20036

White Light Induced E/Z-Photoisomerization of Diphenylamine-tethered Fluorescent Stilbene Derivatives: Synthesis, Photophysical and Electrochemical Investigation

Shachi Mishra[†], Pallavi Awasthi[†], Jagriti Singh[†], Rahul Kumar Gupta[§], Vikram Singh[†], Ruchir Kant[‖], Ram Jeet[†], Debabrata Goswami[§], Atul Goel[*,†,‡]

[†]*Medicinal and Process Chemistry Division, CSIR-Central Drug Research Institute, Lucknow 226031, India;* [§]*Department of Chemistry, Indian Institute of Technology Kanpur, Kanpur 208016, Uttar Pradesh, India;* [‖]*Molecular and Structural Biology Division, CSIR-Central Drug Research Institute, Lucknow 226031, India;* [‡]*Academy of Scientific and Innovative Research, New Delhi 110001, India*

E-mail: atul_goel@cdri.res.in

Table of Contents

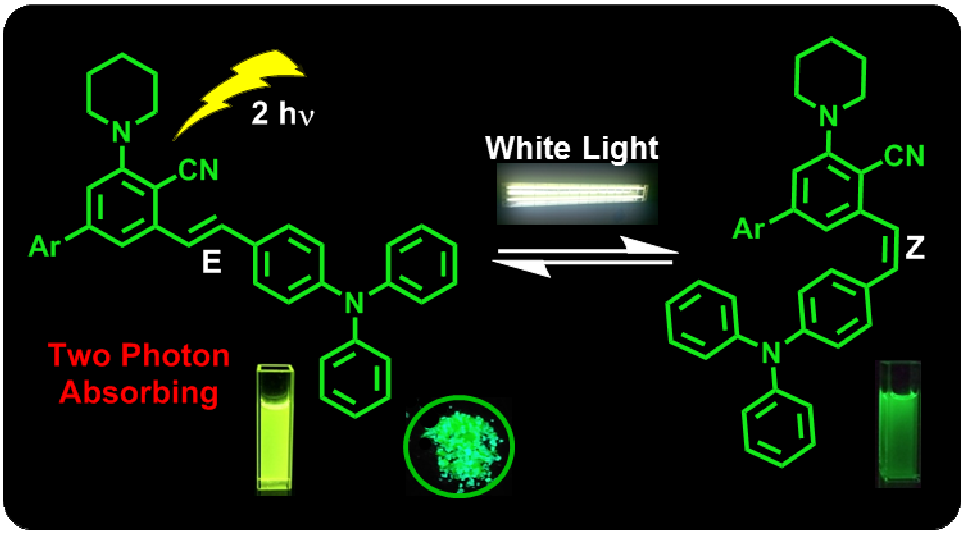

ABSTRACT:

A facile synthesis and detailed photophysical investigation of E/Z-isomerization of fluorescent diphenylamine tethered stilbene derivatives (DPASs) under white light exposure have been carried out to understand the effect on fluorescence, electrochemical properties and photo-stability under various activation/deactivation pathways. In solution state, under dark, E-isomer of DPASs (**6a-d**) exhibited high fluorescence quantum yields ($\Phi_{fl} \approx 53\%$ to 60% in DMSO). However, on white light exposure ^{1}H NMR and HPLC studies revealed that pure E-isomer of the DPAS **6a** (~ 9.5 mM) started converting into its Z-form by photoisomerization until it reaches to nearly equilibrium. At low concentrations (~10 μM), the absorption band of the pure E-isomer in the range of 350-450 nm gradually decreased to adopt Z-conformation **6a′** until a photo-stationary state was reached. The structure of the E-isomer **6a** was unequivocally confirmed by X-ray diffraction analysis. The synthesized DPAS compounds **6a-d** possessed positive solvatochromic properties, two photon absorption properties and good thermal stability. The electrochemical investigations using DPASs showed reversible oxidation resulting in formation of a stable radical cation. Owing to useful photophysical, electrochemical and thermal properties, these DPAS derivatives are suitable for their application in biomedical imaging as well as in fabrication of electroluminescent materials.

INTRODUCTION

The photoinduced E/Z isomerization phenomenon has been an interesting topic in organic and inorganic photochemistry as well as in biology.[1] This phenomenon has been exploited for many applications in photoelectronics, biochemistry and supramolecular chemistry.[2] One of the most fascinating application is the discovery made by the Nobel Laureate G. Wald on the

photochemical E/Z-isomerization of rhodopsin which occurs during the visual cycle.[3] Such molecules have been extensively studied as molecular switches[4], data storage materials,[5] sensors,[6,7] and logic gates.[8] Apart from this, another interesting feature of such molecules is their spectroscopic properties.[9] For better exploration of this feature in biological[10] and optical applications,[11] design and development of stilbene molecules with understanding of stable E/Z configurations are required.

Suitably substituted stilbenes because of their unique charge-transfer characteristics and their utility as promising fluorescent materials have drawn much attention.[12] However, E/Z isomerization reaction of such molecules containing a double bond unit are nearly unavoidable under photo-irradiated conditions in most of the organic molecules[13] and thus limit their use in biomedical and material applications where intense emission is required. Therefore, a detailed study of photoisomerization conditions to get a clear idea about the different energy dissipating processes is necessary. Several reports on stilbene derivatives have been published with or without investigating the E/Z-photoisomerization under normal or UV-visible light (See Supporting Information Table S1).[14] For E/Z-photoisomerisation reactions of di-/triphenylamine tethered stilbene derivatives, most of them have studied the effect on isomerisation upon UV irradiation. However, white light exposure which is unavoidable under working conditions also leads to appreciable E/Z isomerisation reaction and thus a detailed study of stability of E- and Z-isomers under white light exposure is also a prerequisite for design and development of materials for organic photo-electronic applications.

Triphenylamine due to its good electron-donating and transporting capabilities as well as its special propeller starburst molecular structure has been widely used in opto- and electroactive materials.[15] Recently, several diphenylamine based stilbenes have been reported for applications

in OLEDs[16], chemosensors[17] and bio-imaging[18]. The synthetic protocol adopted for these diphenylamine based stilbene derivatives usually involve Wittig reaction, Heck coupling and condensation reactions.[16-18] In this work, we developed a convenient protocol for the synthesis of donor-acceptor π-conjugated diphenylamine based stilbenes through carbanion induced ring transformation reactions at room temperature and studied their optical and photophysical properties in solution and solid state under white light exposure. We further carried out the detailed study of photoisomerization of one of the synthesized dye DPAS **6a** in the presence of white light by using techniques like proton NMR spectroscopy, absorption and emission spectroscopy, quantum mechanical studies and HPLC technique. Electrochemical, thermal and two photon absorption studies were also performed for their useful application in biomedical sciences.

RESULTS AND DISCUSSION

We have previously shown that controlled tuning of π-conjugation and appropriate positioning of D-A moieties modulates dramatically the optical properties of aromatic and heterocyclic compounds.[19,20] Recently, we reported a novel 5,6-dihydro-2*H*-pyrano[3,2-*g*]indolizine (**DPI**) class of luminogens, which exhibited unique solution-solid dual emission (SSDE) behaviour.[21]

The synthetic methodology adopted for the synthesis of designed donor-acceptor (D-A) DPASs is outlined in Scheme 1. The key intermediates 2*H*-pyran-2-ones[19c-e] **3a-d** were prepared from easily accessible precursor substituted acetophenones (**1a-d**) and α-oxo-ketene-*S,S*-acetal (**2**).

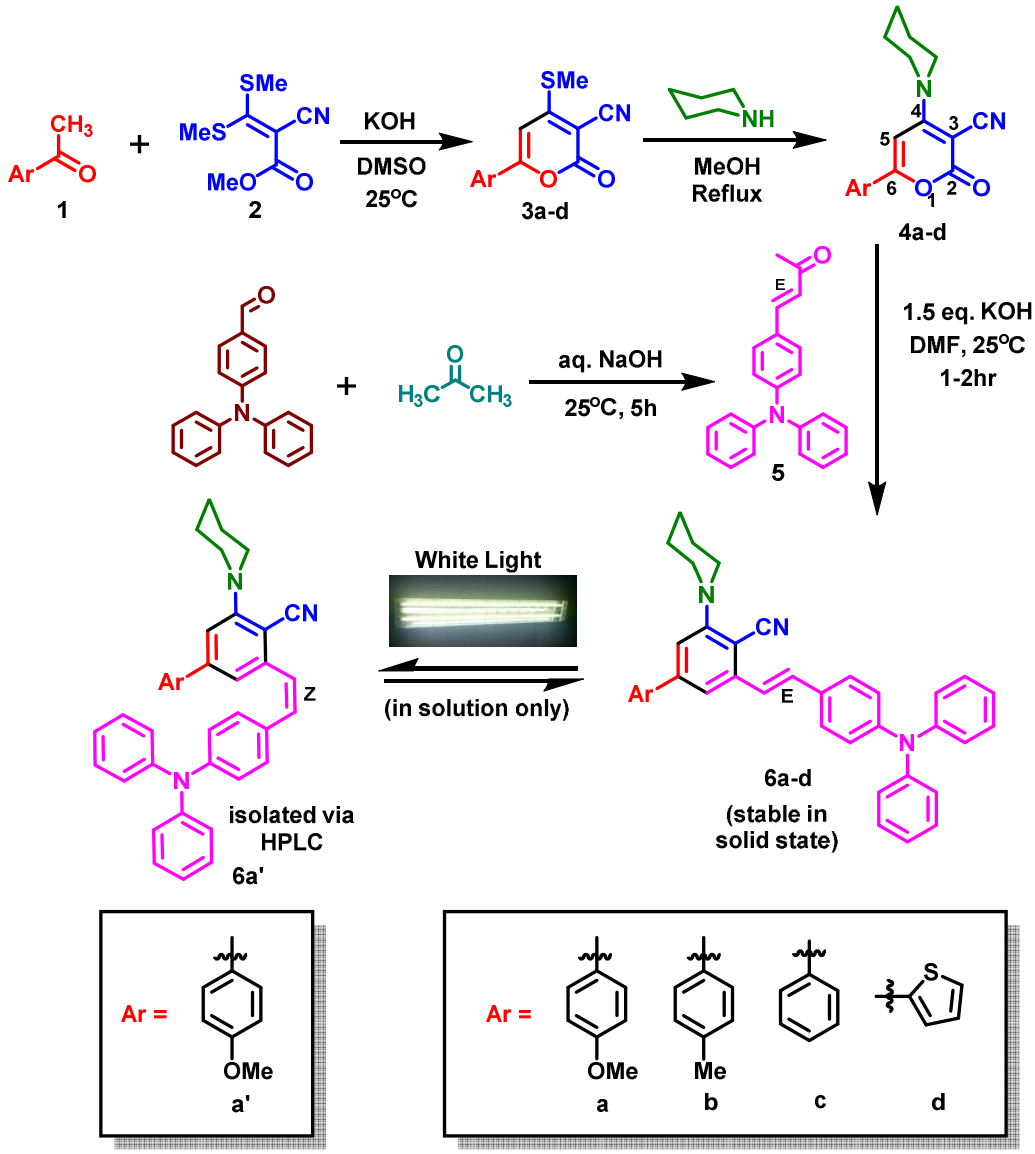

Scheme 1. Synthesis of DPASs **6a–d**

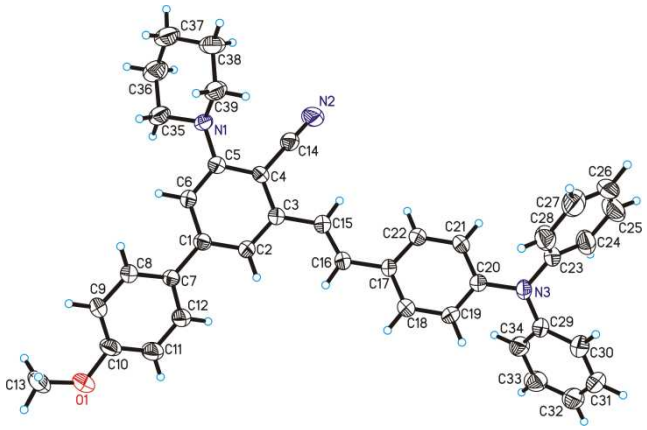

Figure 1. ORTEP diagram drawn with 30% ellipsoid probability for non-H atoms of the crystal structure of compound **6a** determined at 293 K (CCDC No. 1565813).

The methyl sulfanyl group in **3a-d** was replaced by a piperidine donor group to furnish D-A appended 6-aryl-2-oxo-4-piperidin-1-yl-2*H*-pyran-3-carbonitriles (**4a-d**) in good yields.[19c,d,20d] The other precursor (E)-4-(4-(diphenylamino)phenyl)but-3-en-2-one (**5**)[22] was prepared in two steps via formylation of triphenylamine[23] followed by reaction with acetone in good yield (Scheme 1). Further, Michael addition of the conjugate base of **5** to the lactones **4a-d** at position 6 followed by intramolecular cyclization afforded (E)-3-(4-(diphenylamino)styryl)-5-(piperidin-1-yl)biaryl-4-carbonitriles **6a-d**. All of the intermediates and target compounds were characterized by IR, ^{1}H and ^{13}C NMR spectroscopy and mass spectrometry, which confirmed their expected molecular structures. Single crystal X-ray analysis of compound **6a** unambiguously confirmed the structure and the ORTEP drawing is shown in Figure 1.

E/Z Photoisomerization in Solution in the presence and absence (dark) of white light

E/Z isomerization is commonly observed in aromatic and oligomeric olefins, and a detailed study on these type of systems is important to obtain fundamental information about the stability and photophysical properties of the stereoisomers.[24] NMR spectroscopy was used for investigation and confirmation of the E/Z photoisomerization. Starting from solution of pure E-isomer of **6a** (9.5×10^{-3} M in DMSO-d_6), it was observed that when the sample was exposed to white light for few hours, new peaks appeared in the ^{1}H NMR spectrum. Hence, time-dependent NMR analysis was performed to get a clear view. ^{1}H NMR spectra recorded at 0 min was of pure E-isomer with two doublets of J value 16.1 Hz at δ 7.25 and 7.58 ppm (Figure 2). As time elapsed, new peaks emerged which were noticeable after 60 minutes of white light exposure as shown in Figure 2. A new doublet at about δ 6.66 ppm with J value of 12.0 Hz clearly indicated formation of Z-isomer.[25,26] By integrating this signal at 6.66 ppm relative to the constant peak of E-isomer at

7.78 ppm, it was found that the integral of this new isomer increased gradually and reached ~27% relative to the sum of the two isomers after 24h of white light exposure in DMSO-d_6. Further in order to confirm these observations, HPLC analysis of the compound with same concentration in DMSO (9.5 x 10^{-3} M) was carried after 0, 10 and 24 h white light exposure under identical conditions (Figure S1, Supporting Information). It was observed in HPLC that only one additional peak for the Z-isomer with retention time of ~45 min appeared apart from the E-isomer peak (~49 min) on white light exposure. We observed that ~27% of Z-isomer was formed after 24h which is in correlation with the ^{1}H NMR results shown in Figure 2. Furthermore, the HPLC analysis revealed that the photostationary state with ~50% of both E/Z-isomers was achieved after 48 hours of white light exposure (Figure S1, Supporting Information). Interestingly, no isomerization was observed in solution under dark conditions as observed upto 24 h using ^{1}H NMR spectroscopy (Figure S2, Supporting Information).

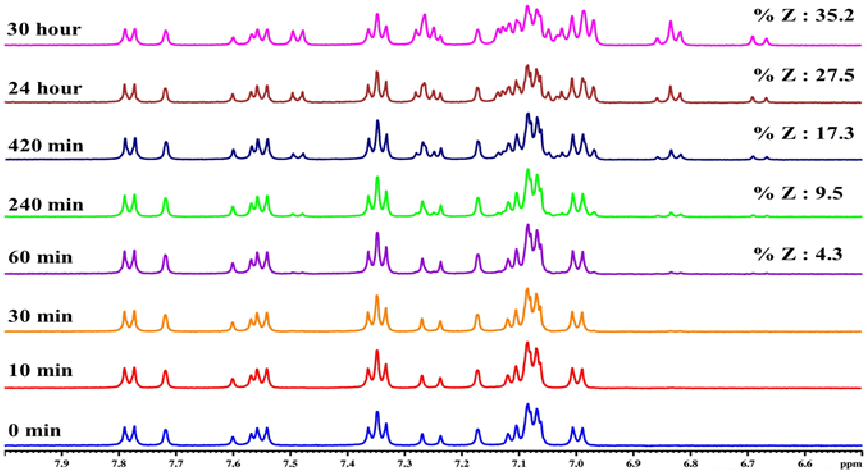

Figure 2. Time dependent ^{1}H NMR of E-isomer on white light exposure

Isolation of Z-6a (6a') from pure E-6a through semi-preparative HPLC

To isolate Z-isomer of **6a** from E-isomer, a solution of **6a** in DCM was exposed to white light and after concentrating, semi-preparative HPLC analysis was carried out as mentioned in

experimental section and the two compounds were isolated. The new compound isolated was characterized by ^{1}H and ^{13}C-NMR spectroscopy and was found to be Z-isomer **(6a′)**. The comparative ^{1}H NMR spectra of E-isomer **(6a)** and Z-isomer **(6a′)** are shown in Figure 3.

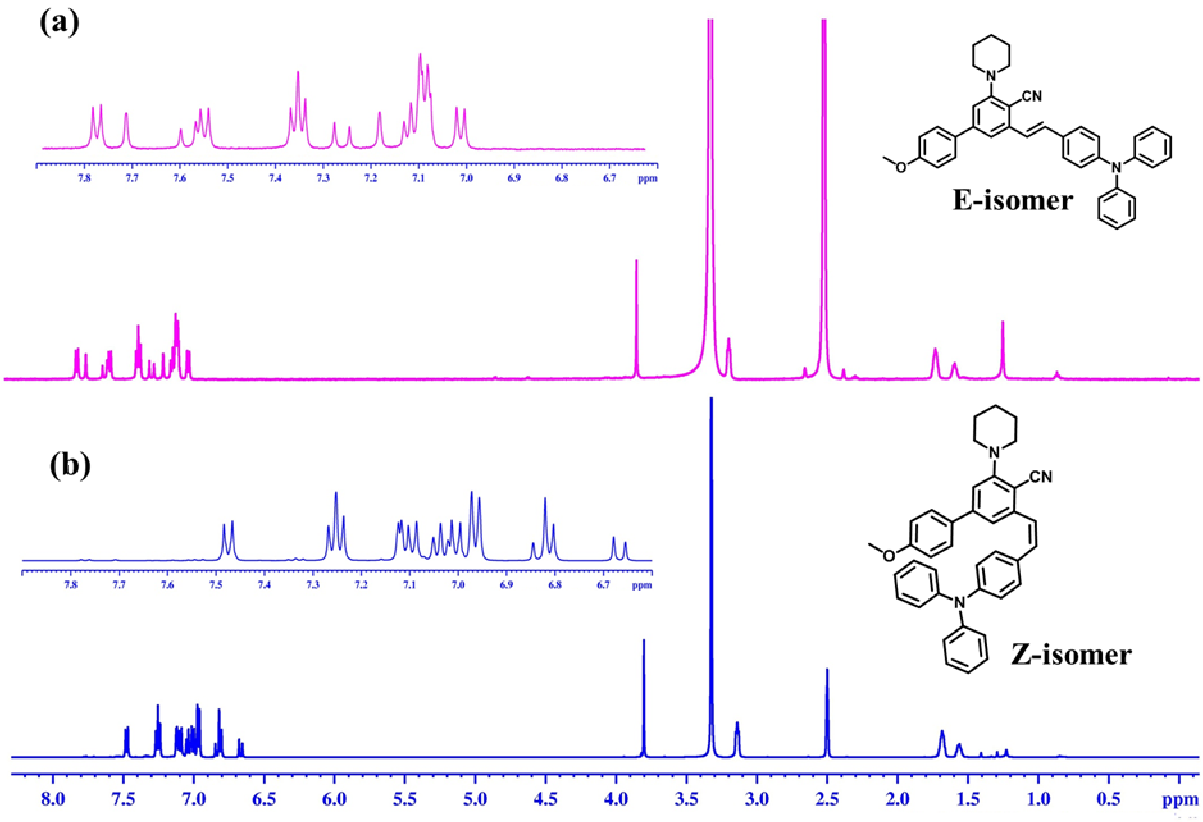

Figure 3. ^{1}H NMR spectra of DPASB (a) **6a (**E-isomer) and (b) **6a′** (Z-isomer) in DMSO-d_6

These experiments (^{1}H NMR and HPLC) clearly implicated that white light plays an important role for driving this isomerisation process in solution state. However, these DPAS compounds are stable in solid state even when exposed to white light for few hours. No isomerisation was observed in solid state upon white light exposure.

Photophysical properties of DPASs 6a-d

The optical properties of the dyes **6a-d** were investigated by measuring absorption and emission spectra in ~10^{-5} M DMSO solutions. The absorption spectra of the dyes are displayed in Figure 4

and the relevant data are listed in Table 1. All the dyes displayed two distinguishable absorption bands. The higher energy absorption band appearing below ~310 nm is assigned to the localized π–π* electronic transitions originating from the triphenylamine chromophores. The lower energy absorption peak at 398-404 nm corresponded to the intramolecular charge-transfer (ICT) electronic transitions from the conjugated segments comprising triphenylamine-styryl-cyano units. All the dyes displayed intense green emission in DMSO (Figure 4 and Table 1) and in the range 480-513 nm in solid state (Table 1 and Figure S3, Supporting Information). E/Z-Isomerization was observed on white light irradiation for all the dyes **6a-d**. Exemplary, detailed investigation of this phenomenon was done for DPAS **6a**.

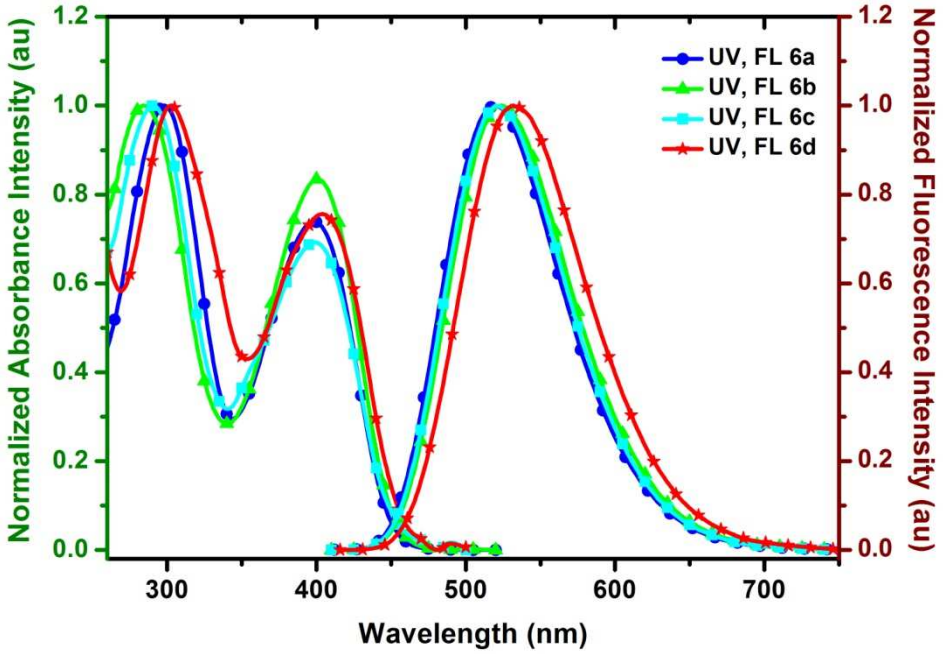

Figure 4. Normalized absorbance and fluorescence spectra of **6a-d** in DMSO (~10^{-5} M).

Table 1. One photon and Two Photon Optical Properties of **6a-d**

entry	$\lambda_{max, abs}$ [a] (nm)	$\lambda_{max, em}$ [b] (nm)	$\lambda_{max, em}$ [c] (nm)	Stokes Shift [d] (cm^{-1})	Φ_f (%) [e]	TPEACS (σ/GM)	
						740 nm [f]	780 nm [f]

6a	298, 398	520	480	5890	57	20.79	13.59
6b	284, 401	523	500	5820	58	nd	10.22
6c	299, 398	520	481	5890	60	11.56	17.35
6d	303, 404	533	513	5990	53	16.46	15.12

[a]Longest-wavelength absorption maximum in DMSO. [b]Fluorescence emission maximum in DMSO. [c]Fluorescence emission maximum in the solid state. [d]Stokes shift (cm^{-1}) = ($1/\lambda_{abs}–1/\lambda_{em}$). [e]Fluorescence quantum yield relative to harmine in 0.1 M H_2SO_4 as a standard (Φ = 45%). σ:Two photon excitation action cross section in GM. [f]Two-photon excitation wavelengths.

Two-Photon Absorption properties of DPASs 6a-d

The two photon excitation action cross-sections of chromophores **6a-d** were measured in the wide wavelength range from 740–785 nm pumped by femtosecond laser pulse at power of 335 mW and keeping the integration time at 300 ms at different excitation wavelengths, exemplary shown for **6a** in Figure 5a and for others in Figure S4, Supporting Information. The two photon excitation action cross section, TPEACS (σ) values are described in Table 1. Figure 5b and Figure S4, Supporting Information shows logarithmic plots of the fluorescence integral versus pumped power with a slope of 1.88, 1.89, 1.95 and 1.73 when the input laser power is increasing, suggesting a two-photon excitation mechanism.

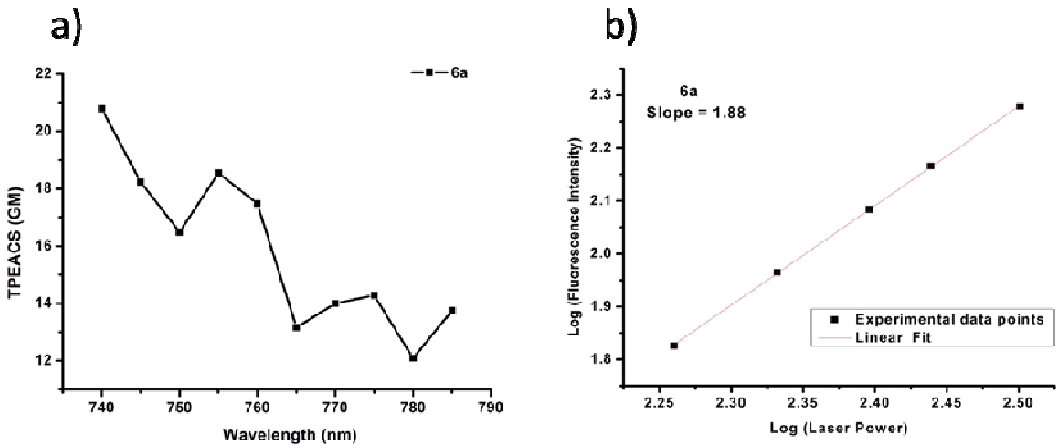

Figure 5. (a) Two photon excitation action cross section (σ, 1 GM = 10^{-50} cm^4 s per photon per molecule) of **6a** in the wavelength region of 740–785 nm at 335 mW. (b) Two-photon absorption verification: Plot of log of Two photon induced fluorescence intensity vs log of laser power of **6a**.

Photophysical studies of E→Z and Z→E isomerisation of 6a :

The E-isomer of DPAS **6a** in DMSO solution (10^{-5} M) exhibited absorption maximum at 299 nm and 398 nm with molar absorption coefficients (ε_{max}) of 34600 M^{-1} cm^{-1} and 26110 M^{-1} cm^{-1} respectively while Z-isomer exhibited an absorption maximum at 299 nm and a shoulder at 356 nm with molar absorption coefficient of 44250 M^{-1} cm^{-1} and 17000 M^{-1} cm^{-1} respectively (Figure 6a, Table 2). The molar absorptivity of the E-isomer at 398 nm was found to be larger than that of the Z-isomer at 356 nm. The peak in E-isomer at 299 nm could be assigned to the local electron transition of triphenylamine group and the peak at 398 nm could be ascribed to the delocalized π to π* transition on the E-stilbene backbone. This second absorption peak was blue shifted (λ_{max} 356 nm) in the case of Z-isomer. These results indicate that there is better ICT character in E-isomer as compared to Z-form, probably due to the twisted conformation of the stilbene moiety in Z-isomer leading to hindrance of the ICT process. Surprisingly, the E-isomer of **6a** showed bright green fluorescence (emission maximum at 522 nm) with good quantum

yield of 57 % in DMSO, while Z-isomer displayed weak fluorescence (emission maximum at 519 nm) with low quantum yield of 4 % (Figure 6b and Table 2).

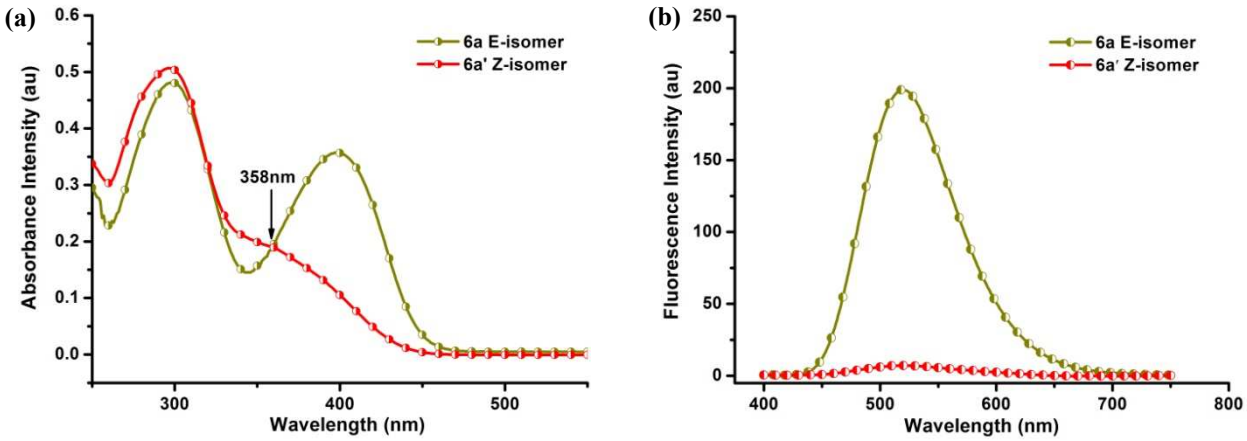

Figure 6. (a) UV-Vis absorption and (b) FL spectra of pure E-(**6a**) and Z-(**6a′**) isomers in DMSO (~10^{-5} M) at room temperature

Table 2: Absorption Properties of **6a** and **6a′**.

entry	$\lambda_{max, abs}$ (nm) (ε_{max}, M^{-1} cm^{-1} X 10^3)[a]	$\lambda_{max, em}$ (nm)[b]	Φ_f (%)[c]
6a-E isomer	298 (34.6), 398 (26.1)	520	57
6a′-Z isomer	299 (44.2), 356 (17.0)	523	4

[a]Longest-wavelength absorption maximum (molar absorptivity) in DMSO. [b]Fluorescence emission maximum in DMSO. [c]Fluorescence quantum yield relative to harmine in 0.1 M H_2SO_4 as a standard (Φ = 45%).

The time-dependent UV-FL studies revealed that pure E-form of **6a** (fluorescence intensity ~200 au) started converting into Z-form (6a') on white light exposure and reached to a stationary state within an hour with fluorescence intensity of ~100 au (Figure 7). Figure 6 and 7a showed the existence of an isobestic point at 358 nm, which indicated that only two species that vary in concentration contribute to the absorbance.[27] Furthermore, a solution of pure Z-isomer was photoisomerized on white light irradiation and in this case, photostationary state was obtained in 30 minutes only, implying thereby that Z-form of **6a** is less stable than E-form (Figure S5 in the Supporting Information). Similar results were obtained for other E-isomer derivatives **6b-d**

(Figure S6 in the Supporting Information). Additionally, we observed that the absorbance of the solution of **6a** (10^{-5} M in DMSO) under continuous monochromatic light exposure at 398 nm for 60 min remained almost constant with respect to time, while the solution of same concentration under white light exposure resulted in significant exponential decrease in absorbance (see Supporting Information Figure S7).

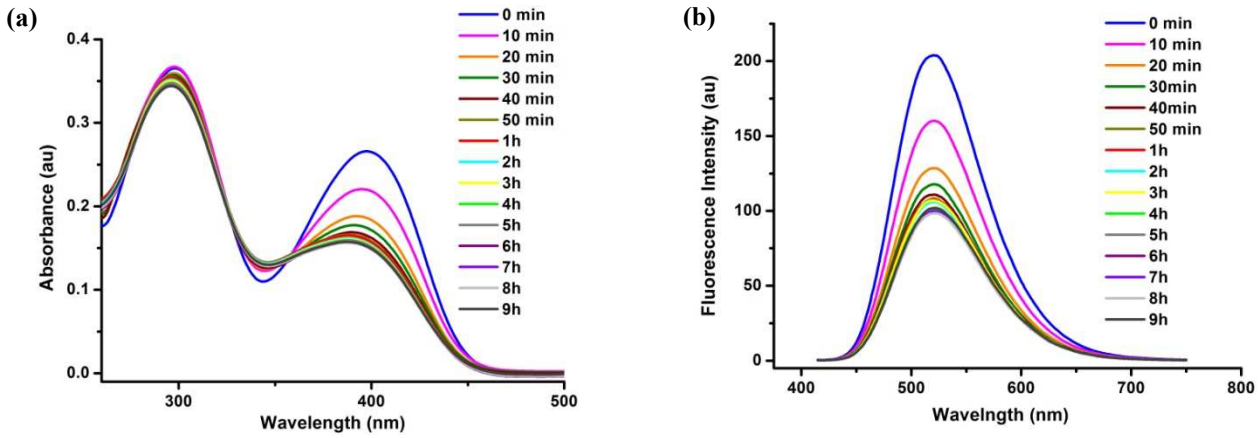

Figure 7. (a) Absorption spectra and (b) Fluorescence spectra of DPASB **6a (E-isomer)** in DMSO (~10^{-5} M) recorded at various times under white light irradiation.

Solvatochromic properties of 6a-d

Molecules with donor-acceptor functionalities are characterized by a prominent solvatochromic effect. Hence, the absorption and emission spectra of E-DPASs in solvents with different polarities were investigated. The photophysical data of all the dyes in different solvents are summarized in Table S2, Supporting Information. The absorption spectra of the dyes **6a-d** are not affected by the solvents of different polarities indicating a non-polar ground state. The one-photon absorption and emission spectra of **6a** in six different solvents are shown in Figure 8 (others in Figure S8, Supporting Information). In the emission spectra, dyes **6a-d** showed a remarkable red shift with solvents of increasing polarity suggesting solvatochromic behaviour of

these DPASs. In order to determine the effect of solvents on E-Z photoisomerisation upon white light exposure, time-dependent UV-Vis spectra of **6a** in different solvents (~10^{-5} M) were investigated. It was observed that E-Z photoisomerisation took place in both non-polar and polar solvents with photostationary state reached within 60 minutes (Figure S9, Supporting Information).

To further evaluate the effect of the solvents on the fluorescence of DPASs, the change in the emission maximum with the Reichardt polarity parameter $E_T(30)$[28] is plotted in Figure 9(a). A linear line with good correlation coefficients (r^2 = 0.99) was obtained, confirming the remarkable solvatochromism of DPASs. Another confirmation regarding the solvent sensitivity of the emission spectra of **6a-d** was obtained by evaluation of its Stokes shift in terms of Lippert–Mataga plot (Figure 9b).[29] For all the dyes, a nice linear correlation (r^2 = 0.98) with respect to the orientation polarizability (Δf) was observed and exhibited a much steeper slope indicating a larger fluorescence solvatochromism. The positive solvatochromism indicated that the donor–acceptor DPASs exhibited a strongly stabilized excited state with high intramolecular charge transfer (ICT) character and larger dipole moments compared to the ground state by the surrounding solvent molecules.

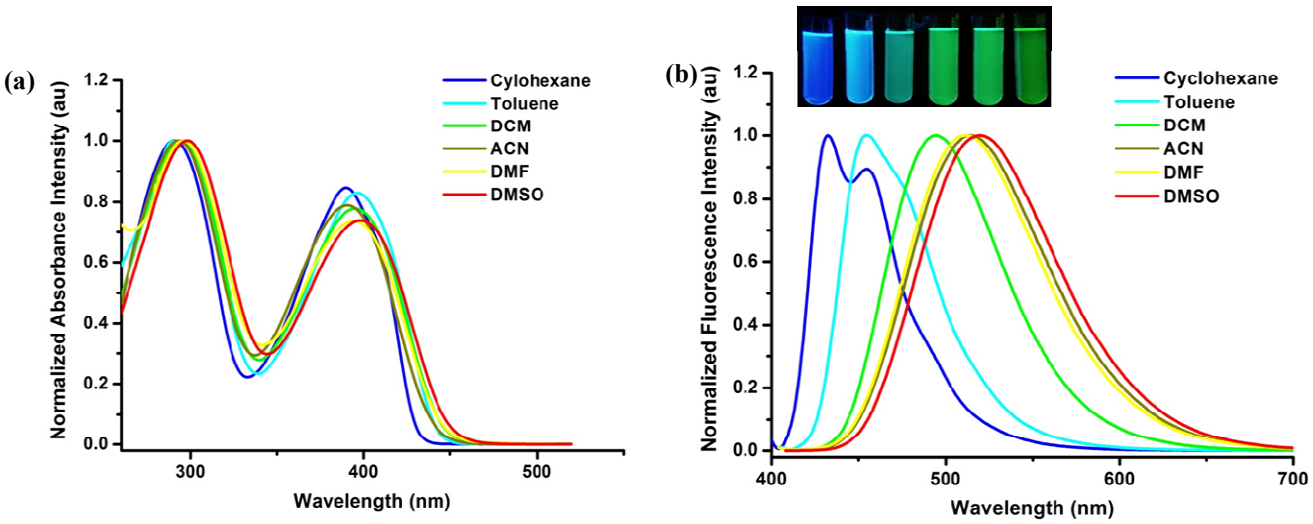

Figure 8. (a) Absorption and (b) emission spectra of dye **6a** in different solvents.

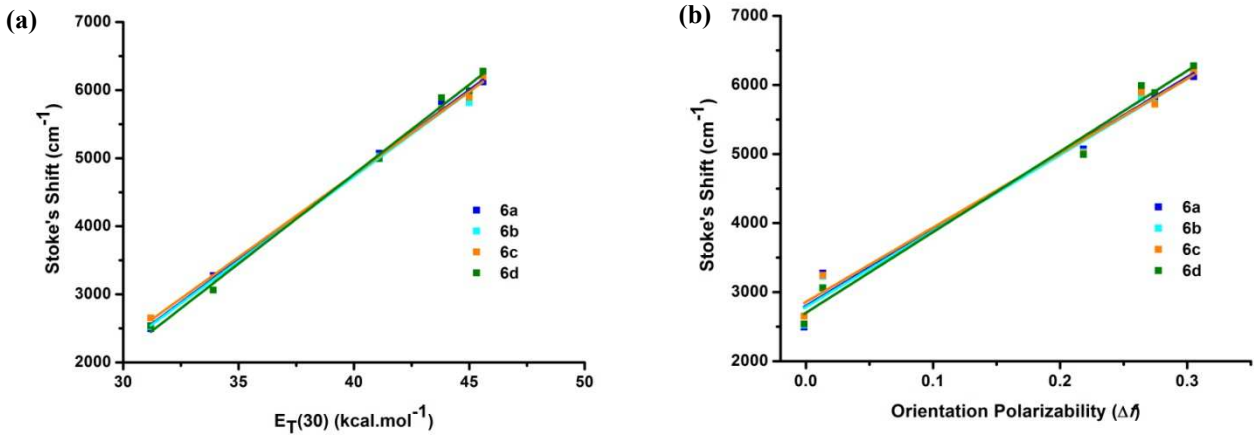

Figure 9. (a) Stokes shift versus $E_T(30)$ and (b) Lippert–Mataga plots of the dyes.

Computational study

To unravel the electronic behaviour of DPASs and to get an insight into the isomerization behaviour**,** the geometry of **6a-d** (E-isomers) was optimized at DFT/B3LYP level using a 6-31G(d,p) basis set and TDDFT calculations was performed using a B3LYP/6-311++G(d,p) method. For E-isomer of **6a,** time-dependent density functional theory (TD-DFT) calculations were carried out taking the coordinates from X-ray data using a B3LYP/6-311++G(d,p) method with a Gaussian 09 package. For all E-isomer derivatives **6a-d**, the HOMO and LUMO values were found to be (-5.19 to -5.25 eV) and (-1.92 to -2.15 eV) respectively (Figure S10 and Table S3, Supporting Information). In all the dyes the longer-wavelength absorption originates from the HOMO to LUMO electronic excitation (Table S3, Supporting Information), which involve a charge migration from the π–conjugated N, N-diphenylaminophenyl (donor) unit to the CN-containing phenyl core segment (acceptor) (Figure S10, Supporting Information).

Comparative analysis of molecular orbitals of **6a** (E-isomer) and **6a'** (Z-isomer) in the ground state are represented in Figure 10. The electronic transition for E-isomer at 427 nm wavelength (HOMO to LUMO) with an oscillator strength (*f*) of 0.7263 corresponded to effective intra-

molecular charge-transfer (ICT) band while for Z-isomer electronic transition at 361 nm wavelength (HOMO to LUMO+1) with an oscillator strength (*f*) of 0.4262 corresponded to less effective intra-molecular charge-transfer (ICT) band than former (Table 3).

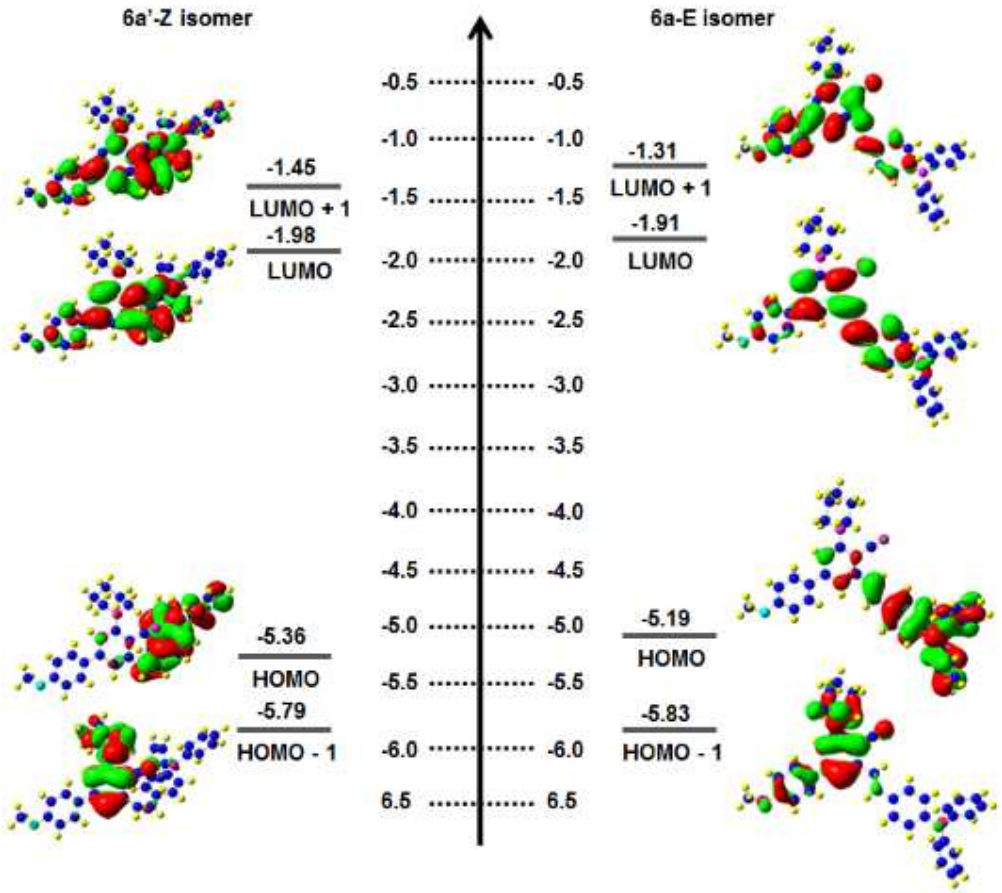

Figure 10. Energy levels and corresponding frontier molecular orbitals of both isomers of **6a** calculated at B3LYP/6-31G* level.

Table 3: Computed Values of Vertical Excitations, Oscillator Strength, Assignment, HOMO, LUMO, and Energy Band Gap of E- and Z-isomer.

entry	$\lambda_{max, abs}$ (nm)	Oscillator Strength (f)	Assignment	HOMO (eV)	LUMO (eV)	E_{0-0} (theoretical)
6a	427	0.7263	HOMO to LUMO (97%)	-5.19	-1.91	3.27
(E-isomer)	375	0.0092	HOMO-1 to LUMO (81%)			
	353	0.1097	HOMO to LUMO+1 (80%)			

6a′	429	0.2395	HOMO to LUMO (96%)	-5.36	-1.98	3.38
(Z-isomer)	387	0.0659	HOMO-1 to LUMO (95%)			
	361	0.4262	HOMO to LUMO+1 (96%)			

Electrochemical and thermal properties

Electrochemical studies were carried out to determine experimental electronic properties of **6a-d**. All measurements were performed in a three-electrode cell setup using Ag/AgCl as reference electrode and a Pt disc as the working electrode, using a 2 mM solution of compound, and 0.2 M of the electrolyte tetrabutylammonium hexafluorophosphate (Bu_4NPF_6) dissolved in DCM. The cyclic voltammograms obtained were employed to evaluate the highest occupied molecular orbital (HOMO) and the lowest unoccupied molecular orbital (LUMO) energy levels (Figure 11a). The HOMO levels were readily estimated from the onset oxidation (E_{ox}) using the equation $E_{HOMO} = -(E_{ox} + 4.8)$ eV, where E_{ox} is the onset oxidation potentials relative to the ferrocene/ferrocenium couple (E_{FOC} = 0.53 V versus Ag/AgCl electrode). The LUMO levels of the dyes were calculated by Eox - $E_{0–0}$, where $E_{0–0}$ is the zeroth–zeroth energy of the dyes estimated from the absorption edge (Table 4). The oxidation processes observed were reversible for **6a-d**, indicating a stable radical cation ion species. Moreover, the highest occupied molecular orbital (HOMO) of DPASs was in the range -5.17 to -5.21 eV, which matched with the work function of indium-tin-oxide (ITO), used as anode in OLED devices.[16c] Hence, DPASs can be utilized as a hole transporting material.

The thermal properties of **6a-d** were gauged by thermogravimetric analysis (TGA) under an argon atmosphere. DPASs **6a-d** were thermally stable up to 368, 357, 368 and 370 °C,

respectively (5% weight loss temperature) as shown in Table 4 and Figure 11b. The good thermal, photophysical and electrochemical properties of these DPASs suggest that these fluorescent compounds are suitable for their application in both biomedical research as well as in fabricating electroluminescent materials.

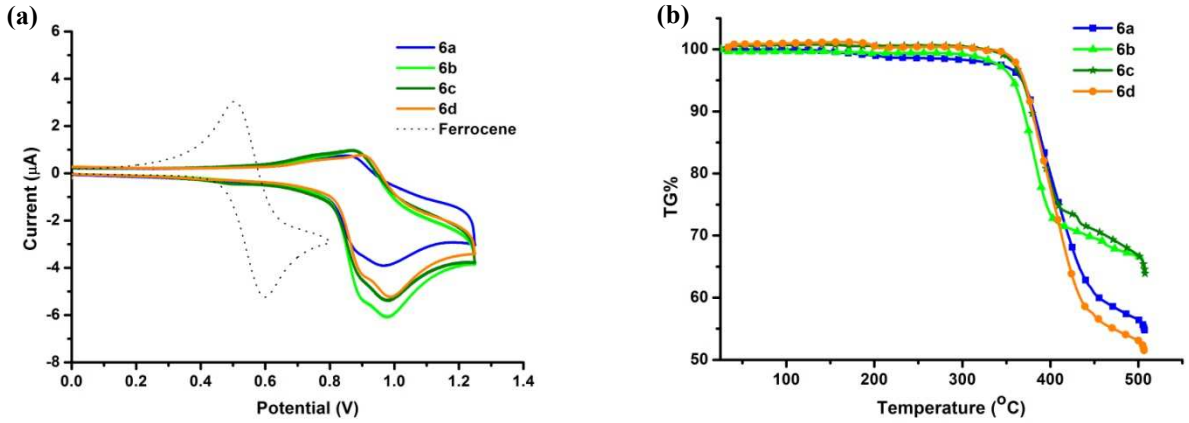

Figure 11. (a) Cyclic voltammograms recorded for compounds **6a-d** in DCM (scan rate = 100 mV/s). (b) Thermogravimetric analysis of compound 6a-d.

Table 4: Electrochemical and thermogravimetric analysis.

entry	T_d[a] (°C)	T_m[b] (°C)	HOMO[c] (eV)	LUMO[d] (eV)	E_{0-0}[e] (eV)
6a	368	218	-5.17	-2.48	2.69
6b	357	197	-5.19	-2.52	2.67
6c	368	208	-5.20	-2.53	2.67
6d	370	200	-5.21	-2.56	2.65

[a]Temperature corresponding to 5% weight loss. [b]Melting temperature gauged by DSC. [c]HOMO = 4.8 + E_{ox}. [d]LUMO = HOMO - E_{0-0}. [e]Optical band gap obtained from the absorption edge.

CONCLUSION

In summary, the E-isomer of diphenylamine–tethered stilbene derivatives (DPASs, **6a-d**) were successfully synthesized using easily accessible precursors through simple reaction conditions. These DPAS derivatives showed good green fluorescence in both solution and solid state with good fluorescence quantum yields (Φ_{fl} ~ 53% to 60% in DMSO). A detailed investigation of the

fluorescence of DPAS **6a** in solution state (~10^{-5} M in DMSO) under white light exposure indicated the formation of E/Z isomerization with a photostationary state being reached after approx. 1 hour under tested conditions. Interestingly, the similar photostationary state with 50 % E/Z-isomers was achieved after 48 hours when DPAS **6a** was analysed by HPLC at higher concentration of approximately 10^{-2} M in DMSO. These data suggested that photoisomerization of DPAS derivatives was concentration dependent and isomerization was faster in dilute solution as compared to concentrated solution. The electrochemical properties of these DPASs showed reversible oxidation process with HOMO values close to work function of indium tin oxide used as anode in OLED devices. These data implicated that DPASs may be used as hole transporting materials in the fabrication of electroluminescent devices. These derivatives also possessed positive solvatochromic properties and two photon absorption properties with good thermal stability. On the basis of such interesting properties and detailed understanding of the photoisomerization phenomenon, these compounds can be applied for material and biological imaging applications.

Experimental Section

General:

^{1}H and ^{13}C NMR spectra were taken at 400 and 500 MHz. $CDCl_3$ and DMSO-d_6 was taken as solvents. Chemical shifts are reported in parts per million shift (δ-value) from Me_4Si (δ 0 ppm for ^{1}H) or based on the middle peak of the solvent ($CDCl_3$) (δ 77.00 ppm for ^{13}C NMR) as an internal standard. Signal pattern are indicated as s, singlet; d, doublet; t, triplet; m, multiplet. Coupling constant (*J*) are given in hertz. Infrared (IR) spectra were recorded in KBr disc and reported in wave number (cm^{-1}). ESIMS spectrometer was used for mass spectra analysis. High

resolution mass spectra were taken with a Q-TOF Analyzer. All the reactions were monitored by TLC and visualization was done by UV-light (254 nm). The purity analysis of the compound was measured using a RP-HPLC and isolation of Z-isomer of **6a** was done using semi-preparative HPLC with the following specification. Analytical HPLC: Shimadzu HPLC (System controller – SCL-10A VP), binary pump (model LC-10AT VP), and detector (SPD-10A VP). Semi-preparative HPLC: Shimadzu HPLC (System controller – CBM-20A (UFLC)), binary pump (model LC-8A), and PDA detector (SPB-M10A VP). Data collection and analysis were performed using Lab solution software. Single crystal X-ray data for compound **6a** was collected on the X-ray diffractometer (Supporting Information Figure S11 and Table S4). The photoisomerization experiments were conducted under white light exposure at room temperature. The "white light" refers to a continuum of wavelengths that is a broad, smooth distribution of photons in the electromagnetic spectrum and is usually emitted by compact fluorescent lamps. During experiments, we simply exposed samples to fluorescent tubes in our lab (commonly used fluorescent tubes for lighting purpose, Crompton Energy Lux FTL, 28W, color temperature 6500K, 220V, light output 2760 Lumen).

Isolation of Z-isomer (6a′) by HPLC technique

Pure E-isomer (**6a**, purity 98.9%, 80mg) was dissolved in DCM to prepare a dilute solution of conc. 10^{-4} M. It was exposed to white light for 48h. Then, DCM was evaporated and dried. Semi-preparative HPLC was done and the system was analyzed in isocratic mode with a mobile phase consisting of acetonitrile–triple distilled water (90:10, v/v) at a flow rate of 0.25 mL min^{-1} and 2.5 mL min-1 respectively. The resolution of both the isomers were achieved using a Phenomenex C18 (5 μm, 4.6 x 250 mm) column for analytical HPLC and YMC-Pack ODS-A

C18 (5 μm, 250 x 20 mm) column for semi-preparative HPLC. The pure Z-isomer (25mg) was obtained in 99% purity and was characterized by ^{1}H and ^{13}C NMR spectroscopy.

Measurement of Two photon absorption properties of DPASs 6a-d

The two-photon excited fluorescence (TPEF) spectra of chromophores **6a-d** were recorded at 740 and 780 nm using mode locked MIRA 900 F (Ti: Saphire) oscillator pumped by Verdi-5 with a pulse duration of 149 fs (integration time 1000 ms) at 76 MHz repetition rate. The TPEF spectral data of **6a-d** was measured in DMSO (c = 1 X 10^{-3} mol L^{-1}) and the reference Rh6G was prepared in methanol (c = 1 X 10^{-3} mol L^{-1}). The TPEACS (Two photon excitation action cross section (σ)) was determined by comparing their two photon excited fluorescence (TPEF) intensity to that of Rh6G, according to the following equation: $\sigma_s = \sigma_r X F_s X \Phi_r X C_r X n_r / F_r X \Phi_s X C_s X n_s$, where the subscripts ''s'' and ''r'' represent sample and reference (here, Rh6G in methanol solution). F is the two-photon excited fluorescence integral intensity of the solution emitted at the exciting wavelength. Φ, n and c are the fluorescence quantum yield, the refractive index of the solvent, and the concentration of the solution, respectively. Values of σ_r are taken from the literature.[30]

Synthesis of (E)-4-(4-(diphenylamino)phenyl)but-3-en-2-one (5). A mixture of 4-(diphenylamino)benzaldehyde (273 mg, 1 mmol, 1 equiv.) in 10% aqueous NaOH with acetone in excess was stirred at 25 ^{o}C for 1 hr. The progress of the reaction was monitored by TLC and on completion the reaction mixture was poured onto crushed ice with vigorous stirring and finally neutralized with 10% HCl. The precipitate 250 mg (91%), obtained was filtered and used for further reactions. Yellow solid, R_f = 0.31(n-hexane/ethyl acetate, 9:1, v/v), Mp: 105^{o}-107^{o}C,

MS (ESI) 314 [M + H^+]. ^{1}H NMR (400 MHz, $CDCl_3$) δ(ppm): 7.44 (d, J = 16.1 Hz, 1H), 7.38 (d, J = 8.6 Hz, 2H), 7.31-7.27 (m, 4H), 7.13-7.07 (m, 6H), 7.00 (d, J = 8.6 Hz, 2H), 6.58 (d, J = 16.1 Hz, 1H), 2.35 (s, 3H). ^{13}C NMR (100 MHz, $CDCl_3$) δ(ppm): 198.3, 150.1, 147.8, 146.7, 143.1, 129.5, 129.4, 129.1, 127.2, 125.4, 124.6, 124.1, 124.0, 122.6, 121.5, 27.3. HRMS (m/z): calcd for $C_{22}H_{20}NO$ $[M+H]^+$ 314.1545, found 314.1543.

General procedure for the synthesis of 4a-d

Compounds **4a-d** were synthesized following previously described synthetic procedures.[19c-e]

Synthesis of (E)-3-(4-(diphenylamino)styryl)-4'-methoxy-5-(piperidin-1-yl)biphenyl-4-carbonitrile (6a). A mixture of 2-oxo-6-(4′-methoxyphenyl)-4-(piperidin-1-yl)-2H-pyran-3-carbonitrile **4a** (620 mg, 2 mmol, 2 equiv.), compound **5** (313 mg, 1 mmol, 1 equiv.), and KOH (112 mg, 2 mmol, 2 equiv.) in dry DMF (10 mL) was stirred at 25 ^{o}C for 1 hr. The progress of the reaction was monitored by TLC and on completion the reaction mixture was poured onto crushed ice with vigorous stirring and finally neutralized with 10% HCl. The precipitate obtained was filtered and purified on a neutral alumina flash column with 2% ethyl acetate in hexane as the eluent to afford 286 mg (51%) as a greenish yellow shiny solid, R_f = 0.41 (n-hexane/ethyl acetate, 8:2, v/v), Mp: 216-218 ^{o}C, MS (ESI) 562 [M + H^+], IR (KBr) ν/cm^{-1}: 2215 (CN). ^{1}H NMR (500 MHz, DMSO-d_6) δ(ppm): 7.78 (d, J = 8.7 Hz, 2H); 7.71(s, 1H), 7.58 (d, J = 16.1 Hz, 1H), 7.55 (d, J = 8.5 Hz, 2H), 7.34 (t, J = 7.8 Hz, 4H), 7.25 (d, J = 16.1 Hz, 1H), 7.17(s, 1H), 7.11-7.06 (m, 8H), 6.99 (d, J = 8.5 Hz, 2H), 3.83 (s, 3H), 3.18 (t, J = 4.7 Hz, 4H), 1.74-1.70 (m, 4H), 1.60-1.56 (m, 2H). ^{13}C NMR (100 MHz, $CDCl_3$) δ(ppm): 160.0, 158.3, 148.2, 147.3, 145.5, 142.8, 132.7, 132.5, 130.3, 129.3, 128.4, 128.0, 124.8, 123.3, 123.2, 123.0, 117.6, 116.1, 115.5, 114.3, 103.7, 55.4, 53.5, 26.1, 24.1. HRMS (m/z): calcd for $C_{39}H_{36}N_3O$ $[M+H]^+$

562.2858, found 562.2849. The X-ray analysis data of **6a** is shown in the Supporting Information Table S4.

Synthesis of (E)-3-(4-(diphenylamino)styryl)-5-(piperidin-1-yl)biphenyl-4-carbonitrile (6b): A mixture of 2-oxo-6-phenyl-4-(piperidin-1-yl)-2H-pyran-3-carbonitrile **4b** (560 mg, 2 mmol, 2 equiv.), compound **5** (313 mg, 1 mmol, 1 equiv.), and KOH (112 mg, 2 mmol, 2 equiv.) in dry DMF (10 mL) was stirred at 25 ^{o}C for 1 hr. The progress of the reaction was monitored by TLC and on completion the reaction mixture was poured onto crushed ice with vigorous stirring and finally neutralized with 10% HCl. The precipitate obtained was filtered and purified on a neutral alumina flash column with 2% ethyl acetate in hexane as the eluent to afford 303 mg (57%) as a greenish yellow shiny solid; R_f = 0.54 (n-hexane/ethyl acetate, 8:2, v/v); Mp: 197-199 ^{o}C; MS (ESI^+) 532 [M + H^+]; IR (KBr) ν/cm^{-1}: 2212 (CN). ^{1}H NMR (400 MHz, $CDCl_3$) δ(ppm): 7.59-7.62 (m, 2H), 7.49- 7.36 (m, 7H), 7.29- 7.20 (m, 6H), 7.13- 7.11 (m, 4H), 7.07-7.03 (m, 5H), 3.20 (t, J = 5.16 Hz, 4H), 1.84-1.79 (m, 4H), 1.65-1.59 (m, 2H). ^{13}C NMR (100 MHz, $CDCl_3$) δ(ppm): 158.2, 148.2, 147.3, 145.9, 142.8, 140.3, 132.6, 130.2, 129.3, 128.9, 128.3, 128.0, 127.2, 124.7, 123.3, 123.0, 122.9, 117.5, 116.5, 116.0, 104.2, 53.5, 26.1, 24.1. HRMS (m/z): calcd for $C_{38}H_{34}N_3$ $[M+H]^+$ 532.2753, found 532.2738.

Synthesis of (E)-3-(4-(diphenylamino)styryl)-4'-methyl-5-(piperidin-1-yl)biphenyl-4-carbonitrile (6c): A mixture of 2-oxo-4-(piperidin-1-yl)-6-p-tolyl-2H-pyran-3-carbonitrile **4c** (598 mg, 2 mmol, 2 equiv.), compound **5** (313 mg, 1 mmol, 1 equiv.), and KOH (112 mg, 2 mmol, 2 equiv.) in dry DMF (10 mL) was stirred at 25 ^{o}C for 1 hr. The progress of the reaction was monitored by TLC and on completion the reaction mixture was poured onto crushed ice with vigorous stirring and finally neutralized with 10% HCl. The precipitate obtained was filtered and purified on a neutral alumina flash column with 2% ethyl acetate in hexane as the eluent to

afford 273 mg (50%) as a greenish yellow solid; R_f = 0.57 (n-hexane/ethyl acetate, 8:2, v/v); Mp: 197-199 ^oC, MS (ESI) 546 [M + H^+], IR (KBr) ν/cm^{-1}: 2214 (CN). ^1H NMR (400 MHz, $CDCl_3$) δ(ppm): 7.51-7.36 (m, 6H), 7.29-7.19 (m, 8H), 7.13-7.03 (m, 9H), 3.19 (t, J = 5.2 Hz, 4H), 2.41 (s, 3H), 1.84-1.78 (m, 4H), 1.64-1.59 (m, 2H). ^{13}C NMR (100 MHz, $CDCl_3$) δ(ppm): 158.2, 148.2, 147.3, 145.8, 142.8, 138.4, 137.4, 132.5, 130.2, 129.6, 129.3, 128.0, 127.1, 124.7, 123.3, 123.1, 122.9, 117.6, 116.3, 115.8, 103.9, 53.5, 26.1, 24.1, 21.1. HRMS (m/z): calcd for $C_{39}H_{36}N_3$ $[M+H]^+$ 546.2900, found 546.2900.

Synthesis of (E)-2-(4-(diphenylamino)styryl)-6-(piperidin-1-yl)-4-(thiophen-2-yl)benzonitrile (6d): A mixture of 2-oxo-4-(piperidin-1-yl)-6-(thiophen-2-yl)-2H-pyran-3-carbonitrile **4d** (586 mg, 2 mmol, 2 equiv.), compound **5** (313 mg, 1 mmol, 1 equiv.), and KOH (112 mg, 2 mmol, 2 equiv.) in dry DMF (10 mL) was stirred at 25 ^oC for 1 hr. The progress of the reaction was monitored by TLC and on completion the reaction mixture was poured onto crushed ice with vigorous stirring and finally neutralized with 10% HCl. The precipitate obtained was filtered and purified on a neutral alumina flash column with 2% ethyl acetate in hexane as the eluent to afford 258 mg (48%) as a yellow shiny solid, R_f = 0.58 (n-hexane/ethyl acetate, 9:1, v/v), Mp: 197-199 ^oC, MS (ESI^+) 539 [M + H^+], IR (KBr) ν/cm^{-1}: 2215(CN). ^1H NMR (400 MHz, $CDCl_3$) δ(ppm): 7.51 (d, J = 1.2 Hz, 1H), 7.46-7.41 (m, 3H), 7.39-7.36 (m, 1H), 7.32-7.19 (m, 7H), 7.14-7.11 (m, 5H), 7.07-7.04 (m, 5H), 3.19 (t, J = 5.2 Hz, 4H), 1.84-1.78 (m, 4H), 1.65-1.60 (m, 2H). ^{13}C NMR (100 MHz, $CDCl_3$) δ(ppm): 158.3, 148.3, 147.3, 143.2, 143.1, 138.7, 132.8, 130.1, 129.3, 128.2, 128.1, 126.4, 124.8, 123.3, 122.9, 122.8, 117.4, 115.1, 114.3, 104.0, 53.4, 26.1, 24.0. HRMS (m/z): calcd for $C_{36}H_{32}N_3S$ $[M+H]^+$ 538.2317, found 538.2309.

(Z)-3-(4-(Diphenylamino)styryl)-4'-methoxy-5-(piperidin-1-yl)biphenyl-4-carbonitrile (6a′): yellow solid, Mp: 87-89 ^{o}C, ^{1}H NMR (500 MHz, DMSO-d_6) δ(ppm): 7.47 (d, J = 8.7 Hz, 2H), 7.25 (t, J = 7.8 Hz, 4H), 7.12-7.08 (m, 4H), 7.05-6.99 (m, 4H), 6.96 (d, J = 7.8 Hz, 4H), 6.84-6.80 (m, 3H), 6.66 (d, J = 12.0 Hz, 1H), 3.80 (s, 3H), 3.13 (t, J = 4.8 Hz, 4H), 1.70-1.66 (m, 4H), 1.58-1.53 (m, 2H). ^{13}C NMR (100 MHz, DMSO-d_6) δ(ppm): 160.2, 158.1, 147.3, 147.3, 147.2, 144.6, 143.2, 133.8, 131.4, 130.5, 130.3, 129.9, 128.5, 126.0, 124.5, 123.8, 122.9, 120.2, 117.6, 115.5, 114.8, 103.4, 55.7, 53.1, 26.2, 24.0. HRMS (m/z): calcd for $C_{39}H_{36}N_3O$ $[M+H]^+$ 562.2858, found 562.2844.

ASSOCIATED CONTENT

Supporting Information

HPLC chromatograms, Time-dependent ^{1}H NMR of **6a** in dark, solid emission spectra of **6a-d**, Two photon absorption spectra, Time-dependent photophysical studies of Z-isomer **6a'** and E-isomers of **6b-d**, Solvatochromic data of **6a-d**, Computational studies of **6a-d** and Cartesian coordinates, X-ray data of **6a** and NMR spectra of **5**, **6a**, **6a′**, **6b-d**. This material is available free of charge via the Internet at http://pubs.acs.org.

AUTHOR INFORMATION

Corresponding Author

*E-mail: atul_goel@cdri.res.in

Notes

The authors declare no competing financial interest.

ACKNOWLEDGEMENTS

AG thanks the Department of Atomic Energy (DAE-SRC) for Outstanding Investigator Award (21/13/2015-BRNS/35029). SM, PA, JS and RKG are thankful to UGC, DST and CSIR, New Delhi, India for research fellowships. We thank Dr. Tejender S. Thakur for supervising the X-ray Data collection and structure determination of the compound reported in this paper. We are grateful to Dr. R. Ampapathi for his help in obtaining time-dependent NMR spectra and SAIF-CDRI, Lucknow, India for providing other spectral and analytical data. CDRI communication number is 9648.

REFERENCES

(1) (a) Wald, G. *Science* **1968**, *162*, 230-239. (b) Oesterhelt, D.; Stoeckenius, W. *Nature* **1971**, *233*, 149-152. (c) Oesterhelt, D.; Stoeckenius, W. *Proc. Natl. Acad. Sci.* **1973**, *70*, 2853-2857 (d) Braun, A. M.; Maruette, M. T.; Oleveros, E. *Photochemical Technology*, Wiley, New York, **1991**, Chapter 12, pp. 500.

(2) Bandara, H. M. D.; Burdette, S. C. *Chem. Soc. Rev.*, **2012**, *41*, 1809–1825.

(3) (a) Durr, H.; Bous-Laurent, H. *Photochromism: Molecules and systems*, Elsevier, Amsterdam **1990** (b) Feringa, B. L. *Tetrahedron* **1993**, *49*, 8267-8270.

(4) Guo, X.; Zhou, J.; Siegler, M. A.; Bragg, A. E.; Katz, H. E. *Angew. Chem. Int. Ed.* **2015**, *54*, 4782–4786.

(5) (a) Wang, Y.; Tan, X.; Zhang, Y. M.; Zhu, S.; Zhang, I.; Yu, B.; Wang, K.; Yang, B.; Li, M.; Zou, B.; Zhang, S. X. A. *J. Am. Chem. Soc.* **2015**, *137*, 931–939. (b) Leblond, J.; Gao, H.; Petitjean, A.; Leroux, J.-C. *J. Am. Chem. Soc.* **2010**, *132*, 8544–8545.

(6) Xu, Z.; Singh, N. J.; Lim, J.; Pan, J.; Kim, H. N.; Park, S.; Kim, K. S.; Yoon, J. *J. Am.*

Chem. Soc. **2009**, *131*, 15528–15533.

(7) (a) Ling, J.; Naren, G.; Kelly, J.; Moody, T. S.; de Silva, A. P. *J. Am. Chem. Soc.*, **2015**, *137*, 3763–3766. (b) Li, K.; Xiang, Y.; Wang, X.; Li, J.; Hu, R.; Tong, A.; Tang, B. Z. *J. Am. Chem. Soc.*, **2014**, *136*, 1643–1649.

(8) Qu, D.-H.; Wang, Q.-C.; Tian, H. *Angew. Chem. Int. Ed.*, **2005**, *44*, 5296–5299.

(9) Dekhtyar, M.; Rettig, W. *J. Phys. Chem. A*, **2007**, *111*, 2035–2039. (b) Lapouyade, R.; Kuhn, A.; Letard, J.-F.; Rettig, W. *Chem. Phys. Lett.*, **1993**, *208*, 48–58.

(10) (a) Choi, S; Tong Ong, D. S.; Kelly, J. W. *J. Am. Chem. Soc.*, **2010**, *132*, 16043–16051. (b) Tian, F.; Debler, E. W.; Millar, D. P.; Deniz, A. A.; Wilson, I. A.; Schultz, P. G. *Angew. Chem. Int. Ed.*, **2006**, *45*, 7763–7765.

(11) Cariati, E.; Cavallo, G.; Forni, A.; Leem, G.; Metrangolo, P.; Meyer, F.; Pilati, T.; Resnati, G.; Righetto, S.; Terraneo, G.; Tordoin, E. *Cryst. Growth Des.*, **2011**, *11*, 5642–5648.

(12) (a) Zhang, X.; Zhang, X.; Tao, L.; Chi, Z.; Xu,J.; Wei, Y. *J. Mater. Chem. B*, **2014**, *2*, 4398–4414. (b) Hu, R.; Lam, J. W. Y.; Deng, H.; Song, Z.; Zheng, C.; Tang, B. Z. *J. Mater. Chem. C*, **2014**, *2*, 6326–6332.

(13) (a) Birks, J. B. *Chem. Phys. Lett.* **1976**, *38*, 437–440. (b) Orlandi, G.; Siebrand, W. *Chem. Phys. Lett.* **1975**, *30*, 352–354.

(14) (a) Li, W.; Wang, S.; Zhang, Y.; Gao, Y.; Dong, Y.; Zhang, X.; Song, Q.; Yang, B.; Ma, Y.; Zhang, C. *J. Mater. Chem. C*, **2017**, *5*, 8097-8104. (b) Bejarano, F.; Alcon, I.; Crivillers, N.; Mas-Torrent, M.; Bromley, S. T.; Veciana, J.; Rovira, C. *RSC Adv.*, **2017**, *7*, 15278–15283. (c) Gapol, M. A. B.; Balanay, M, P.; Kim, D. H. *J. Phys. Chem. A* **2017**, *121*, 1371−1380. (d) Gautam, P.; Yu, C. P.; Zhang, G.; Hillier, V. E.; Chan, J. M. W. *J. Org. Chem.* **2017**, *82*, 11008−11020. (e) Yu, C. Y. Y.; Xu, H.; Ji, S.; Kwok, R. T. K.; Lam, J. W. Y.; Li, X.; Krishnan,

S.; Ding, D.; Tang, B. Z. *Adv. Mater.* **2017**, *29*, 1606167. (f) Aich, K.; Das, S.; Gharami, S.; Patra, L.; Mondal, T. K. *New J. Chem.*, **2017**, *41*, 12562-12568. (g) Zhang, Y.; Li, H.; Zhang, G.; Xu, X.; Kong, L.; Tao, X.; Tiana, Y.; Ya, J. *J. Mater. Chem. C* **2016**, *4*, 2971-2978. (h) Zhao, M.; Zhu, Y.; Su, J.; Geng, Q.; Tian, X.; Zhang, J.; Zhou, H.; Zhang, S.; Wu, J.; Tian, Y. *J. Mater. Chem. B,* **2016***, 4*, 5907-5912 (i) Campos, R. I.; Wu, X.; Elgland, M.; Konradsson, P.; Hammarström, P. *ACS Chem. Neurosci.* **2016**, *7*, 924−940. (j) Kong, M.; Wang, T.; Tian, X.; Wang, F.; Liu, Y.; Zhang, Q.; Wang, H.; Zhou, H.; Wu, J.; Tian, Y. *J. Mater. Chem. C,* **2015**, *3*, 5580-5588. (k) Yang, Y.; Liu, F.; Wang, H.; Bo, S.; Liu, J.; Qiu, L.; Zhena, Z.; Liu, X. *J. Mater. Chem. C*, **2015**, *3*, 5297-5306. (l) Wang, S.; Xu, H.; Yang, Q.; Song, Y.; Li, Y. *RSC Adv.*, **2015**, *5*, 47990–47996. (m) Liu, Y.; Kong, M.; Zhang, Q.; Zhang, Z.; Zhou, H.; Zhang, S.; Li, S.; Wu, J.; Tian, Y. *J. Mater. Chem. B*, **2014**, *2*, 5430-5440. (n) Lai, H.; Xiao, Y.; Yan, S.; Tian, F.; Zhong, C.; Liu, Y.; Weng, X.; Zhou, X. *Analyst*, **2014**, *139*, 1834–1838. (o) Yang, M.; Xu, D.; Xi, W.; Wang, L.; Zheng, J.; Huang, J.; Zhang, J.; Zhou, H.; Wu, J.; Tian, Y. *J. Org. Chem.* **2013**, *78*, 10344−10359. (p) Lin, C. -K.; Prabhakar, C.; Yang, J. –S. *J. Phys. Chem. A* **2011**, *115*, 3233–3242. (q) Tian, H.; Yang, X.; Chen, R.; Zhang, R.; Hagfeldt, A.; Sun, L. *J. Phys. Chem. C*, **2008**, *112*, 11023-11033. (r) Allain, C.; Schmidt, F.; Lartia, R.; Bordeau, G.; Fiorini-Debuisschert, C.; Charra, F.; Tauc, P.; Teulade-Fichou, M. –P.; *ChemBioChem* **2007**, *8*, 424 – 433. (s) Miljanić, S.; Frkanec, L.; Meić, Z.; Žinic, M. *Eur. J. Org. Chem.* **2006**, 1323–1334 (t) Yang, J. –S.; Chiou, S. –Y.; Liau, K. –L. *J. Am. Chem. Soc.* **2002**, *124*, 2518-2527.

(15) (a) Ning, Z. J.; Tian, H. *Chem. Commun.* **2009**, 5483-5495. (b) Liu, B.; Zhang, Q.; Ding, H. J.; Wu, J. Y.; and Tian, Y. P. *Dyes Pigm*. **2012**, *95*, 149-160.

(16) (a) Xu, T.; Yang, M.; Liu, J.; Wu, X.; Murtaza, I.; He, G.; Meng, H. *Org. electron.* **2016**, *37*, 93-99. (b) Huang, F.; Zhang, Y.; Liu, M. S.; Cheng, Y.-J.; Jen, A. K.-Y. *Adv. Funct. Mat.*

2007, *17*, 3808-3815. (c) Wei, M.; Huang, R.; Guo, K.; Jing, Y.; Xu, T.; Wei, B. *J. Mat. Chem. C* **2014**, *2*, 8131-8136.

(17) (a) Juang, R.-S.; Wen, H.-W.; Chen, M.-T., Yang, P.-C. *Sens. Actuators, C* **2016**, *231*, 399-411. (b) Koersten, S.; Mohr, G. J. *Chem. Eur. J.* **2011**, *17*, 969-975. (c) Liu, T.; Huo, F.; Yin, C.; Li, J.; Chao, J.; Zhang, Y. *Dyes Pigm*. **2016**, *128*, 209-214.

(18) (a) Gan, X.; Ge, X.; Zhai, C.; Zheng, J.; Tang, X.; Yang, Y.; Tian, Y.; Zhang, X.; Zhou, H. *Dyes Pigm*. **2017**, *138*, 7-14. (b) Ding, A.-X.; Hao, H.-J.; Gao, Y.-G.; Shi, Y.-D.; Tang, Q.; Lu, Z.-L. *J. Mat. Chem. C* **2016**, *4*, 5379-5389.

(19) (a) A. Goel, A. Sharma, M. Rawat, R. S. Anand, and R. Kant *J. Org. Chem.* **2014**, 79, 10873-10880. (b) Goel, A.; Dixit, M.; Chaurasia, S.; Kumar, A.; Raghunandan, R.; Maulik, P. R.; Anand, R. S. *Org. Lett.*, **2008**, *12*, 2553-2556. (c) Goel, A.; Chaurasia, S.; Dixit, M.; Kumar, V.; S.; Prakash, S.; Jena, B.; Verma, J. K.; Jain, M.; Anand, R. S.; Manoharan, S. S. *Org. Lett.*, **2009**, *11*, 1289-1292. (d) Goel, A.; Sharma, A.; Kathuria, M.; Bhattacharjee, A.; Verma, A.; Mishra, P. R.; Nazir, A.; Mitra, K. *Org. Lett.*, **2014**, *16*, 756-759.

(20) (a) Sharma, A.; Umar, S.; Kar, P.; Singh, K.; Sachdev, M.; Goel, A. *Analyst*, **2016**,*141*, 137-143. (b) Goel, A.; Umar, S.; Nag, P.; Sharma, A.; Nazir, A.; Kumar, L.; Shamsuzzama; Gayen, J. R.; Hossain, Z. *Chem. Commun.* **2015**, *51*, 5001-5004. (c) Jha, A. K.; Umar, S.; Arya, R. K.; Datta, D.; Goel, A. *J. Mater. Chem. B*, **2016**, *4*, 4934-4940.

(21) Raghuvanshi, A.; Jha, A. K.; Sharma, A.; Umar, S.; Mishra, S.; Kant, R.; Goel, A. *Chem. Eur. J.*, **2017**, *23*, 4527-4531.

(22) Mizuyama, N.; Murakami, Y.; Nagaoka, J.; Kohra, S.; Ueda, K.; Hiraoka, K.; Shigemitsu, Y.; Tominaga,Y. *Heterocycles* **2006**, *68*, 1105-1108.

(23) Fox, C. J.; Johnson, A. L. *J. Org. Chem.*, **1964**, *29*, 3536–3538.

(24) (a) Baik, C.; Hudson, Z. M.; Amarne, H.; Wang, S. *J. Am. Chem. Soc.* **2009**, *131*, 14549 – 14559 (b) Arai, T.; Karatsu, T.; Sakuragi, H.; Tokumaru, K. *Tetrahedron Lett.* **1983**, *24*, 2873 – 2876.

(25) Jędrzejewska, B.; Ośmiałowskia, B.; Zaleśny, R. *Photochem. Photobiol. Sci.* **2016**, *15*, 117–128.

(26) (a) *Introduction to NMR spectroscopy*, 2nd ed.; Abraham, R. J., Fisher, J., Loftus, P., Eds.; Wiley: Chichester, U.K., 1988. (b) Lambert, J. B.; Shurvell, H. F.; Lightner, D. A.; Cooks, R. C. *Organic Structural Spectroscopy*; Prentice Hall: Upper Saddle River, NJ, 1998.

(27) Amine Fourati, M.; Skene, W. G.; Géraldine Bazuin, C.; Prud'homme, R. E. *J. Phys. Chem. A* **2013**, *117*, 836−844.

(28) Reichardt, C. *Angew. Chem. Int. Ed*. **1979**, *18,* 98-110.

(29) (a) Lippert, E. V. *Z. Elektrochem.* **1957**, *61*, 962–975. (b) Mataga, K. N.; Kaifu, Y.; Koizumi, M. *Bull. Chem. Soc. Jpn.* **1956**, *29*, 465–470.

(30) Xu, C.; Webb, W. W. *J. Opt. Soc. Am. B*, **1996**, *13*, 481–491.